this stress and cause the irradiated endothelial cells to transfer. These movements seemed to influence the leakage of heat stress and made it difficult to diminish gene induction in nontargeted cells. Furthermore, applying the irradiating IR laser to the tissue resulted in intense heating of the elliptic region elongated vertically just before the focus,[9] suggesting that the muscle cells located in the vertical region of the optical axis were easily influenced by the laser. We attempted some modification of the IR-LEGO system by interrupting the center of the irradiated laser before focusing and tried to reduce the leakage to the surrounding cells in the vertical region. Eliminating ectopic heating will require further improvements to the optical system in the IR-LEGO system. In contrast, we were able to achieve deletion of gene expression in the nontargeted cells from another viewpoint by using tissue-/cell-specific promoters and a recombination system. We then attempted to use the Cre-loxP system[3] to reduce the minor leakage in nontargeted cells and establish double-transgenic zebrafish line with *hsp:Cre* and *kdrl:loxP:nlsGFP:loxP:mCherry* (the promoter of the *kdrl* gene also induces gene expression specifically in the endothelial cells). Using the embryos from these transgenic organisms, we noted that laser-mediated induction of the Cre gene only influenced the endothelial cells, in which the downstream effecter of loxP sequence could be expressed by genome recombination of Cre. These improvements will elevate the value of IR-LEGO system as the precise in vivo gene regulation method in near future.

Because we succeeded in identifying the optimized condition of irradiation, we tried to label and trace the single endothelial cells of the first SeAs to elucidate their contribution to the connection between the vascular systems of the brain and spinal cord (Figure 3D and 3E). The tracing experiment with IR-LEGO system revealed that these endothelial cells bridged the BA to DLAV, and suggested that this system was valuable for fate-mapping analysis. We were able to trace strong mCherry expression in the targeted cells for >48 hours after induction. Lineage tracing analysis with time-lapse imaging of the *fli1:nEGFP* transgenic zebrafish was used to determine the source of the lymphatic endothelial cells to the thoracic duct.[13] Although tracing backward in time the particular nucleus in time-lapse sequences was a useful method, the range of tracing the targeted cells was restricted to the imaging view. Transplantation of labeled cells or the labeling of individual cells by injecting heritable dye has been also used for tracing analysis and has provided useful products.[14] However, these methods have been applied to the embryos only up to the mid-to-late blastula stages. In contrast, our method using the IR-LEGO system has no limitations for tracing the range and developmental stage, and therefore, it will be a powerful tool to map the fate of various cell types at later stages and to analyze the distribution or function of tissue-specific stem cells in various tissues, such as the digestive system.

Using the water heating property of the IR laser effectively, an overdose of laser irradiation was able to ablate the targeted cells. We ablated the endothelial cells of the first SeAs and assessed its influence on the connecting vessels between the brain and spinal cord. On the irradiated side, the connection between the BA and DLAV diminished, and the PHBC did not connect to the DLAV (Figure 4A and 4B). This suggested the primary role of the first SeA in bridging BA and PHBC to DLAV, and the ablation experiment was a valuable method for analyzing the influence of the particular vessel on vascular morphogenesis.

By tracing and ablating the cells of the first SeAs, we clearly indicated their contribution to the connection between the vascular systems of the brain and spinal cord in zebrafish. In contrast, Padget[15] precisely described how these vascular systems were constructed by reconstructing serial sections of human embryos. In human embryos, the PHBC was identified at the 20-somite stage; the bilateral longitudinal neural arteries subsequently formed in the ventromedial region. Bilateral longitudinal neural arteries were medially fused to form the BA and were subsequently connected to the first SeAs. A zebrafish does not have a neck, and the final vascular systems in this region may greatly differ from those in human beings. However, the early processes, during which these vasculatures form, progress in a manner highly similar to that observed in humans; therefore, we believe that zebrafish can be considered a useful model to analyze the vascular formation between the brain and spinal cord. We are now very interested in the guidance mechanisms surrounding vascular formation in this region and are focusing on the perivascular tissues, such as the pericytes and mesenchymal cells, as well as the neural tissue. The IR-LEGO system will help us address this issue.

We demonstrated that the IR-LEGO system is a powerful tool with the potential to contribute to developmental biology. However, there are some limitations to this system. The most critical limitation is the depth of targeted cells. We achieved a maximum induction rate of 60% for the targeted single endothelial cells in the intersegmental vessels, which are usually located at a depth of 50 to 60 μm. The endothelial cells of the first SeA were localized at a depth of ≈70 μm, which might cause a decrease in the efficiency of inducing gene expression in the tracing experiment. We assume that the limitation of gene induction in the single cells is at a depth of ≈100 μm. The IR-LEGO system can be applied to various tissues at later developmental stages; however, the targeted region is restricted to a depth of 100 μm. We also indicated that the IR-LEGO system is useful for the ablation of single cells. Combining the ablation study with time-lapse imaging enables us to observe the regeneration process of ablated tissues. Induction of regeneration-associated genes after ablation will also contribute to understanding the underlying mechanisms.

In this study, we applied the IR-LEGO system to vascular biology and succeeded in demonstrating its usability in zebrafish. Our method enabled gene induction in single endothelial cells, tracing of targeted cells by fluorescent proteins, and ablation of the targeted vessel. Inducing the genes associated with vascular formation will help us to investigate the regulation of vascular connections. Furthermore, combined with small interfering RNA-mediated gene suppression, IR-LEGO will enable in vivo gene manipulation with vertebrate model organisms, and it leads to the prospect of uncovering the mechanisms underlying vascular morphogenesis.

Acknowledgments

We thank Dr Brant Weinstein (National Institutes of Health) for the transgenic zebrafish strain and Dr Ryozo Nagai (Jichi Medical

University) for proofreading the article. We also thank Mutsumi Kurosawa, Taro Ando, Yohei Sawa, Yuki Matsumoto, and Motohiko Koizumi (Iwate Medical University) for the technical support offered for the screening and bleeding of the transgenic zebrafish, and we thank Misako Saida-Taniguchi (National Institute for Basic Biology) for offering technical support in optics.

Sources of Funding

This work was carried out under the National Institute for Basic Biology Cooperative Research Program (11-336) for E. Kimura and was supported by Grants-in-Aid for Scientific Research (KAKENHI) of Japan Society for the Promotion of Science (JSPS) grant number 23590222 (E. Kimura).

Disclosures

None.

References

1. Risau W. Mechanisms of angiogenesis. *Nature*. 1997;386:671–674.
2. Isogai S, Lawson ND, Torrealday S, Horiguchi M, Weinstein BM. Angiogenic network formation in the developing vertebrate trunk. *Development*. 2003;130:5281–5290.
3. Lakso M, Sauer B, Mosinger B Jr, Lee EJ, Manning RW, Yu SH, Mulder KL, Westphal H. Targeted oncogene activation by site-specific recombination in transgenic mice. *Proc Natl Acad Sci USA*. 1992;89:6232–6236.
4. Sato Y, Watanabe T, Saito D, Takahashi T, Yoshida S, Kohyama J, Ohata E, Okano H, Takahashi Y. Notch mediates the segmental specification of angioblasts in somites and their directed migration toward the dorsal aorta in avian embryos. *Dev Cell*. 2008;14:890–901.
5. Halloran MC, Sato-Maeda M, Warren JT, Su F, Lele Z, Krone PH, Kuwada JY, Shoji W. Laser-induced gene expression in specific cells of transgenic zebrafish. *Development*. 2000;127:1953–1960.
6. Ramos DM, Kamal F, Wimmer EA, Cartwright AN, Monteiro A. Temporal and spatial control of transgene expression using laser induction of the hsp70 promoter. *BMC Dev Biol*. 2006;6:55.
7. Feder ME, Hofmann GE. Heat-shock proteins, molecular chaperones, and the stress response: evolutionary and ecological physiology. *Annu Rev Physiol*. 1999;61:243–282.
8. Sato-Maeda M, Tawarayama H, Obinata M, Kuwada JY, Shoji W. Sema3a1 guides spinal motor axons in a cell- and stage-specific manner in zebrafish. *Development*. 2006;133:937–947.
9. Kamei Y, Suzuki M, Watanabe K, Fujimori K, Kawasaki T, Deguchi T, Yoneda Y, Todo T, Takagi S, Funatsu T, Yuba S. Infrared laser-mediated gene induction in targeted single cells in vivo. *Nat Methods*. 2009;6:79–81.
10. Deguchi T, Itoh M, Urawa H, et al. Infrared laser-mediated local gene induction in medaka, zebrafish and Arabidopsis thaliana. *Dev Growth Differ*. 2009;51:769–775.
11. Isogai S, Horiguchi M, Weinstein BM. The vascular anatomy of the developing zebrafish: an atlas of embryonic and early larval development. *Dev Biol*. 2001;230:278–301.
12. Hosokawa Y, Ochi H, Iino T, Hiraoka A, Tanaka M. Photoporation of biomolecules into single cells in living vertebrate embryos induced by a femtosecond laser amplifier. *PLoS One*. 2011;6:e27677.
13. Yaniv K, Isogai S, Castranova D, Dye L, Hitomi J, Weinstein BM. Live imaging of lymphatic development in the zebrafish. *Nat Med*. 2006;12:711–716.
14. Kimmel CB, Warga RM. Tissue-specific cell lineages originate in the gastrula of the zebrafish. *Science*. 1986;231:365–368.
15. Padget DH. The development of the cranial arteries in the human embryo. *Contrib Embryol*. 1948;212:207–260.

Significance

In vivo spatiotemporal gene regulation in a single cell is obligatory to analyze specific gene functions associated with morphogenesis in developing embryos. The infrared laser–evoked gene operator system is a new microscopic method optimized to heat cells by using an IR laser, which has a superior ability to heat water and can efficiently access deep-lying tissues. We applied this method to the vascular system in zebrafish embryos and first succeeded in gene induction driven by heat shock promoter in the targeted endothelial cells. Inducing the particular genes using this method will help us to investigate the particular gene function in vivo. Additionally, combined with small interfering RNA-mediated gene suppression, infrared laser–evoked gene operator will enable in vivo gene manipulation in the future. Our achievement in this study will lead us to the prospect of uncovering the mechanisms underlying morphogenesis of vertebrate model organisms.

J Neurol (2012) 259:1698–1705
DOI 10.1007/s00415-011-6402-5

ORIGINAL COMMUNICATION

Fractional anisotropy in the centrum semiovale as a quantitative indicator of cerebral white matter damage in the subacute phase in patients with carbon monoxide poisoning: correlation with the concentration of myelin basic protein in cerebrospinal fluid

Takaaki Beppu · Shunrou Fujiwara · Hideaki Nishimoto · Atsuhiko Koeda · Shinsuke Narumi · Kiyoshi Mori · Kuniaki Ogasawara · Makoto Sasaki

Received: 23 October 2011 / Accepted: 26 December 2011 / Published online: 19 January 2012

Abstract Carbon monoxide (CO) poisoning leads to demyelination of cerebral white matter (CWM) fibers, causing chronic neuropsychiatric symptoms. To clarify whether fractional anisotropy (FA) from diffusion tensor imaging in the centrum semiovale can depict demyelination in the CWM during the subacute phase after CO inhalation, we examined correlations between FA in the centrum semiovale and myelin basic protein (MBP) in cerebrospinal fluid. Subjects comprised 26 adult CO-poisoned patients ≤60 years old. MBP concentration was examined for all patients at 2 weeks after CO inhalation. The mean FA of the centrum semiovale bilaterally at 2 weeks was also examined for all patients and 21 age-matched healthy volunteers as controls. After these examinations, the presence of chronic symptoms was checked at 6 weeks after CO poisoning. Seven patients displayed chronic symptoms, of whom six showed abnormal MBP concentrations. The remaining 19 patients presented no chronic symptoms and no abnormal MBP concentrations, with MBP concentrations undetectable in 16 patients. The MBP concentration differed significantly between patients with and without chronic symptoms. The mean FA was significantly lower in patients displaying chronic symptoms than in either patients without chronic symptoms or controls. After excluding the 16 patients with undetectable MBP concentrations, a significant correlation was identified between MBP concentration and FA in ten patients. The present results suggest that FA in the centrum semiovale offers a quantitative indicator of the extent of demyelination in damaged CWM during the subacute phase in CO-poisoned patients.

Keywords Carbon monoxide poisoning · Cerebral white matter fiber · Demyelination · Diffusion tensor imaging · Fractional anisotropy · Myelin basic protein

Abbreviation

CNS	Central nervous system
CSF	Cerebrospinal fluid
CO	Carbon monoxide
COHb	Carboxyhemoglobin
DNS	Delayed neuropsychiatric sequelae
DTI	Diffusion tensor imaging
FA	Fractional anisotropy
ADC	Apparent diffusion coefficient
GCS	Glasgow coma scale
MBP	Myelin basic protein

T. Beppu (✉) · S. Fujiwara · H. Nishimoto · K. Ogasawara
Department of Neurosurgery, Iwate Medical University, Uchimaru 19-1, Morioka 020-8505, Japan
e-mail: tbeppu@iwate-med.ac.jp

T. Beppu
Department of Hyperbaric Medicine, Iwate Medical University, Uchimaru 19-1, Morioka 020-8505, Japan

A. Koeda
Department of Psychiatry, Iwate Medical University, Uchimaru 19-1, Morioka 020-8505, Japan

S. Narumi
Department of Neurology, Iwate Medical University, Uchimaru 19-1, Morioka 020-8505, Japan

K. Mori
Iwate Prefectural Advanced Critical Care and Emergency Center, Morioka, Japan

M. Sasaki
Advanced Medical Research Center, Iwate Medical University, Morioka, Japan

MRI Magnetic resonance imaging
ROI Region of interest
T2WI T2-weighted magnetic resonance imaging

Introduction

Approximately 30% of patients surviving acute carbon monoxide (CO) poisoning display various chronic neuropsychiatric symptoms [31, 32]. Of these, approximately two-thirds demonstrate persistent neurological symptoms from the acute phase to the chronic phase. The remaining one-third show delayed neuropsychiatric sequelae (DNS), which are recurrent neuropsychiatric symptoms occurring after an interval of apparent normality ("lucid interval;" mean duration 22 days) following apparent recovery from acute symptoms [6, 33]. Animal experiments and some clinical studies have led to the hypothesis that damage after CO poisoning results from complicated mechanisms due to CO-mediated toxicity: mitochondrial oxidative stress in the central nervous system (CNS) following CO-induced tissue hypoxia [35]; perivascular oxidative stress mediated by intravascular neutrophil activation [26]; and alteration of myelin basic protein (MBP), a major myelin component in the CNS, due to lipid peroxygenation leading to auto-immunological demyelination of CNS [24, 25]. Auto-immunological demyelination induces further inflammation in the cerebral white matter (CWM) [31]. Gray matter structures, such as the cerebral cortex, basal ganglia and hippocampus, must be damaged by severe hypoxia, since these structures display higher cellular activity and higher oxygen requirements than white matter structures and are more vulnerable to oxygen deprivation [29]. However, damage in the CWM is seen in patients both with and without damage to gray matter structures, and the severity of CWM damage appears to correlate with prognosis in CO-poisoned patients [15, 34].

Assessment of CWM damage caused by CO poisoning in the acute or subacute phase contributes to predictions of progress to DNS and prognosis of chronic symptoms, and appropriate triage of patients with CO poisoning for observation and treatment. Additional quantitative and objective examinations are desirable for assessment of CWM damage after CO poisoning. However, no universally accepted severity scale in routine examinations, such as level of consciousness or carboxyhemoglobin concentration, is available for assessing CWM damage caused by CO poisoning. This is because clinical features are largely affected by the degree of cellular hypoxia resulting from binding of CO to myoglobin rather than hemoglobin and may be markedly affected by various conditions before admission, such as the duration before hospitalization and the care provided before hospitalization [7, 12, 20]. As one of mechanisms for damage in CWM is auto-immunological demyelination, measuring the MBP concentration in the cerebrospinal fluid (CSF) has recently been proposed as an indicator for the extent of CWM damage after CO poisoning [11, 14]. However, detection of MBP using a lumbar tap is a highly invasive procedure and only indicates white-matter damage somewhere within the entire CNS. A less-invasive, objective and quantitative examination that could be used in place of measuring MBP is therefore desired. Diffusion tensor imaging (DTI), a magnetic resonance imaging (MRI) sequence, is potentially more sensitive for detecting demyelination in CWM. Among various quantitative parameters such as apparent diffusion coefficient (ADC) and eigenvalues derived from DTI, fractional anisotropy (FA) has been recognized as the most useful for evaluating the integrity of CWM fibers [2]. Indeed, FA is frequently used for evaluating the extent of damaged CWM fibers in patients with demyelinating diseases such as multiple sclerosis [1, 27]. CO poisoning causes damage in various regions of the CWM, but the centrum semiovale has been considered a region more responsible for chronic neuropsychiatric symptoms after CO poisoning than other regions [4, 10, 19, 22]. Herein, we measured FA from DTI at the centrum semiovale in CO-poisoned patients, and evaluated the correlation between the FA and concentration of MBP in the CSF. This study aimed to clarify whether FA in the centrum semiovale offers a quantitative indicator of the extent of demyelination in damaged CWM during the subacute phase in CO-poisoned patients.

Methods

Patients

All study protocols were approved by the Ethics Committee of Iwate Medical University, Morioka, Japan. Patients recruited to this study were admitted to Iwate Medical University Hospital between April 2008 and February 2011. Entry criteria for this study were: age $\geq$20 but $\leq$60 years in patients who had suffered from CO poisoning caused by a fire or charcoal burning; performance of DTI and measurement of MBP concentration according to the protocol in this study; no past history of brain disorders, including surgical operation, irradiation, stroke, infection or demyelinating disease; and provision of written informed consent to participate. Diagnosis was based on present history of exposure to CO and presence of acute neurological symptoms such as impairment of consciousness and headache on admission. After excluding patients

who did not meet the entry criteria, 26 patients were enrolled. Mean duration from the scene of CO exposure to arrival at our institute was 5.0 h (range 0.3–81 h). All patients were treated with hyperbaric oxygenation therapy (HBO_2) (60 min of 100% oxygen inhalation via mask at 2.8 atmospheres absolute) started within 24 h of admission. HBO_2 was continued with a single daily session for a week excluding the weekend. HBO_2 was further continued for 4–8 weeks in cases with persistent symptoms. If DNS occurred, HBO_2 was restarted and continued until 2 months after CO exposure. HBO_2 was discontinued upon patient request or when symptoms were sufficiently improved. Duration of HBO_2 administration for all patients ranged from 1 to 60 sessions (mean 12 sessions). The day of CO inhalation was defined as day 1 in this study.

Measurement of MBP concentration in CSF

MBP concentration in the CSF was examined using a lumbar tap at 2 weeks after CO poisoning (between day 12 and day 16) for all patients. Obtained CSF was frozen at −20°C within 1 h after lumbar tap, then the frozen CSF was transported on dry ice to an outside laboratory (SRL, Tokyo, Japan). MBP in the CSF was assayed and measured using a MBP ELISA kit (Cosmic Corp., Tokyo, Japan) immediately after arrival at the laboratory. If the assay was delayed for a long time, frozen CSF was stored at −80°C. An abnormal MBP concentration was defined as ≥102 pg/ml. When the level of MBP was below the limit of detection, the result from the laboratory was reported as MBP ≤40 pg/ml.

DTI

For all patients, DTI was also performed at 2 weeks (between day 12 and day 16) using a 3.0-T whole-body scanner (GE Yokogawa Medical Systems, Tokyo, Japan) and 8-channel coil. Measurements of FA and ADC were performed using data from DTI (repetition time, 10,000 ms; echo time, 62 ms; matrix 128 × 128; field of view, 240 × 240 mm; 4 mm thickness with 1.5 mm gap; 6 motion-probing gradient directions; b value, 1,000 s/mm^2). The region of interest (ROI) was manually placed in the bilateral centrums semiovale in the CWM on non-diffusion-weighted images (Fig. 1). FA and ADC were measured bilaterally at the centrum semiovale, using free MRIcro software (http://www.cabiatl.com/mricro/). The FA and ADC for each subject were determined as the mean of values measured twice by the same investigator (S.F.), who was blinded to clinical data. The second measurement was performed 1 week after the first test, using a different randomized order of measurements from the first test.

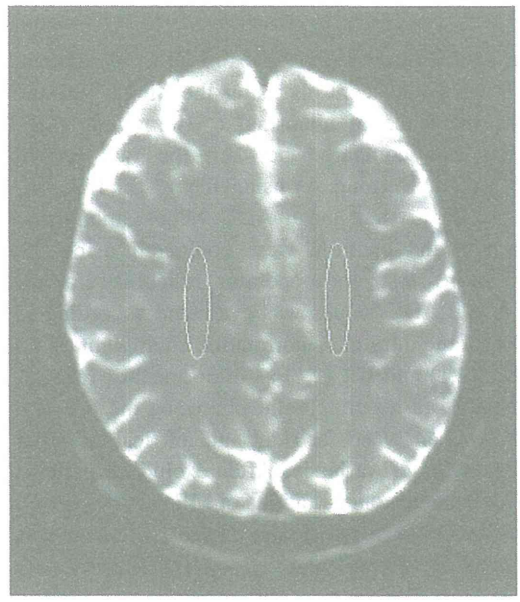

Fig. 1 Measurements of FA and ADC value at the centrum semiovale in a patient (case 7 in group S). Regions of interest (ROIs) were placed bilaterally on the centrum semiovale in non-diffusion-weighted image

Finally, the mean FA and mean ADC values for the right and left centrum semiovale were calculated and defined as absolute values for each subject. The same procedures described above were performed for 21 age-matched healthy volunteers as controls (18 men, 3 women; mean age 41 ± 10 years, range 22–56 years).

Observation of symptoms

Neurological symptoms were continuously observed for 6 weeks after admission using routine neurological examinations. Patients were assigned to one of two groups according to clinical behavior at 6 weeks (day 40–44) after CO poisoning: group S, patients displaying neuropsychiatric symptoms; group A, patients showing asymptomatic status. Group S included both patients with symptoms persisting for 6 weeks and patients with DNS. DNS was defined as recurrent symptoms after apparent improvement of acute symptoms followed by a lucid interval. General intellectual function was also estimated using the mini-mental state examination (MMSE) [9] at 6 weeks after CO exposure. We defined the normal range, borderline range and dementia according to MMSE scores as ≥27, ≤26 but ≥22, and ≤21, respectively. When scores were considered borderline, patients with educational background ≥9 years and evidence of obvious personality change according to interviews with family members were diagnosed with dementia.

Statistical analyses

We statistically compared differences in mean age among group S, group A and controls using the Mann-Whitney U test. The incidence of abnormal (≥102 pg/ml) MBP concentration was compared between the two patient groups (group S and group A) using the χ^2 for independence test. Mean FA and mean ADC values among two patients groups and controls were compared using the Mann-Whitney U test. Intra-operator reliability for all absolute FA and ADC values was evaluated according to classification of the intra-class correlation coefficient (ICC) [21]. For ICC(1,1) and ICC(1,k) as intra-operator reliability, agreement of all absolute values between the first and second tests was analyzed for right and left lesions using one-factor analysis of variance. After excluding patients showing undetectable concentrations of MBP (≤40 pg/ml), the correlation between MBP and mean FA value was estimated using Spearman's correlation coefficient by rank test. Statistical significance was established at the $p < 0.05$ level in all analyses.

Results

A total of 51 patients were admitted to our institute for treatment of CO poisoning between April 2008 and February 2011. After excluding 25 patients who did not meet the entry criteria for this study, a total of 26 patients (24 men, 2 women; mean age 40.1 ± 11.4 years) were enrolled. All patient data are summarized in Table 1. In 19 (73%) of 26 patients, acute symptoms resolved completely within 4 days after admission, and no neuropsychiatric symptoms were present at 6 weeks from CO-inhalation (group A). The remaining seven patients (27%) displayed chronic neuropsychiatric symptoms at 6 weeks (group S), including four patients with continuous persistence of symptoms for 6 weeks and three patients exhibiting DNS

Table 1 Summary of all patients

Case	Group	Age	Etiology	COHb (%)	GCS	MBP (pg/ml)	Mean FA	Mean ADC	Main symptom at 6 weeks	MMSE score
1	S	29	Suicide	24.8	11	252	0.345	0.622	Dementia (persistent)	23
2	S	57	Suicide	25.1	10	176	0.344	0.548	Parkinsonism (persistent)	27
3	S	38	Suicide	1.5	6	468	0.239	0.494	Apallic syndrome (persistent)	NS
4	S	55	Suicide	39.7	3	376	0.346	0.548	Dementia (persistent)	16
5	S	56	Suicide	13.5	11	130	0.338	0.584	Akinetic mutism (DNS)	NS
6	S	29	Suicide	3.6	14	99	0.353	0.498	Parkinsonism (DNS)	28
7	S	48	Suicide	28.6	6	110	0.317	0.565	Dementia (DNS)	23
1	A	22	Suicide	20.5	15	52.8	0.488	0.492	None	29
2	A	31	Suicide	47.3	13	40.6	0.354	0.494	None	30
3	A	22	Suicide	9.3	12	63.6	0.447	0.555	None	30
4	A	47	Heating	33.3	14	≤40	0.441	0.496	None	30
5	A	44	Heating	13.7	15	≤40	0.388	0.528	None	30
6	A	26	Suicide	1.9	15	≤40	0.395	0.504	None	30
7	A	47	Heating	22.6	14	≤40	0.393	0.551	None	29
8	A	28	Suicide	19.2	15	≤40	0.440	0.521	None	30
9	A	41	Suicide	2.7	11	≤40	0.381	0.487	None	30
10	A	55	Heating	14.0	13	≤40	0.366	0.504	None	30
11	A	35	Suicide	25.3	8	≤40	0.425	0.497	None	30
12	A	56	Suicide	12.2	15	≤40	0.395	0.501	None	30
13	A	36	Suicide	44.1	12	≤40	0.398	0.513	None	30
14	A	34	Suicide	31.0	12	≤40	0.394	0.530	None	30
15	A	57	Heating	40.1	13	≤40	0.400	0.541	None	30
16	A	32	Suicide	19.3	10	≤40	0.358	0.509	None	30
17	A	34	Suicide	38.6	5	≤40	0.406	0.535	None	30
18	A	36	Suicide	23.5	10	≤40	0.358	0.520	None	30
19	A	48	Suicide	44.0	6	≤40	0.352	0.539	None	30

COHb and GCS indicate results of the initial examination

COHb carboxyhemoglobin, *GCS* Glasgow coma scale, *NS* no study performed because of unconsciousness

after apparent improvement of acute symptoms followed by a lucid interval. DNS in three patients occurred after DTI and measurement of MBP on day 21 in case 5, day 19 in case 6 and day 18 in case 7. Mean age was 45 ± 12 years in group S, 38 ± 11 years in group A and 41 ± 10 years in controls. No significant differences in age were found between groups S and A ($p = 0.24$), between group S and controls ($p = 0.51$), or between group A and controls ($p = 0.40$).

In the seven patients in sroup S, six showed abnormal MBP concentrations (≥102 pg/ml), and one patient showed a level of 99 pg/ml. None of the 19 patients in group A showed abnormal concentrations of MBP, with 16 patients showing undetectable concentrations of MBP (≤40 pg/ml). The incidence of an abnormal MBP levels was statistically different between groups P and A ($p < 0.001$). MBP concentrations for the four patients with persistent symptoms in group S, for the three patients with DNS in group S and for the three patients in group A were more than ≥150 pg/ml, around 100 pg/ml and around 50 pg/ml, respectively (Table 1).

Table 2 shows ranges and means of FA and ADC for each group. The range of FA for group S slightly overlapped that for group A, but differed markedly from that for controls. Ranges of FA for group A and controls were similar. The mean FA for group S was significantly lower than those for group A ($p < 0.001$) and controls ($p < 0.001$), whereas no significant difference was found between group A and controls ($p = 0.57$) (Fig. 2a). In Fig. 2a, individual mean FA values of the three patients with DNS were not obviously different from those of the four patients with persistent symptoms in group S. Group S patients were clearly differentiated from group A patients at a cutoff of 0.353 (100% sensitivity, 94.7% specificity) and from controls at a cutoff of 0.360 (100% sensitivity, 100% specificity). On the other hand, the range of ADC in each group was similar, and the mean ADC did not differ significantly among any of the three groups (Fig. 2b). Intra-operator reliability for absolute FA was classified as "almost perfect" for the centrum semiovale bilaterally; ICC(1,1) and ICC(1,*k*) were 0.88 and 0.93 for the right side, and 0.95 and 0.98 for the left side, respectively. Intra-operator reliability for absolute ADC was also classified as "almost perfect" for bilateral centrum semiovale; ICC(1,1) and ICC(1,*k*) were 0.98 and 0.99 for the right side, and 0.91 and 0.95 for the left side, respectively.

After excluding 16 patients showing undetectable levels (≤40 pg/ml), the ten remaining patients (all patients in groups S and 3 patients in group A) showed a strong correlation between the mean FA and MBP ($r = -0.79$, $p = 0.02$) (Fig. 3).

Discussion

Ide et al. [11] have documented that MBP concentration in patients with DNS showed marked elevation around 2 weeks after CO poisoning, peaking at around 30 days.

Table 2 Range and mean value of FA and ADC for each group

	FA		ADC ($\times 10^{-3}$ mm^2/s)	
	Range	Mean	Range	Mean
Group S	0.239–0.353	0.326 ± 0.040	0.494–0.622	0.551 ± 0.045
Group A	0.352–0.447	0.395 ± 0.029	0.487–0.601	0.517 ± 0.021
Controls	0.363–0.445	0.400 ± 0.027	0.472–0.580	0.517 ± 0.023

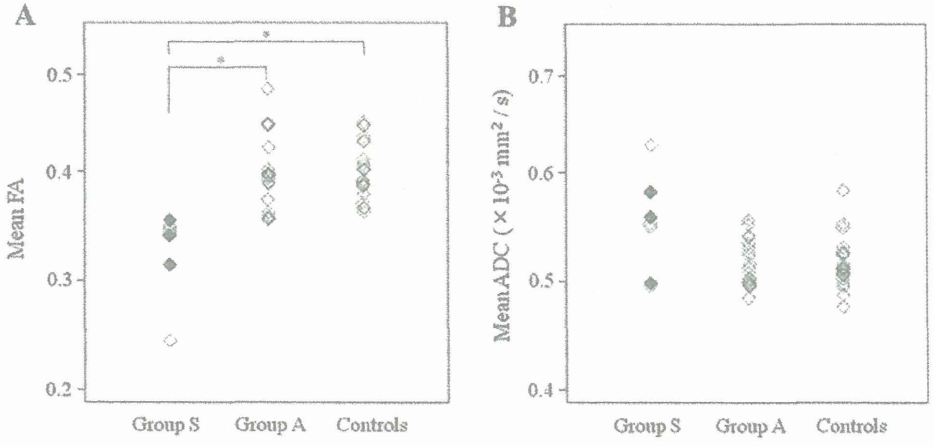

Fig. 2 Differences of mean FA (**a**) and mean ADC (**b**) values in the centrum semiovale bilaterally among group S, group A and controls. In group S, *black and white squares* represent patients with DNS and persistent symptoms, respectively (*$p < 0.001$).

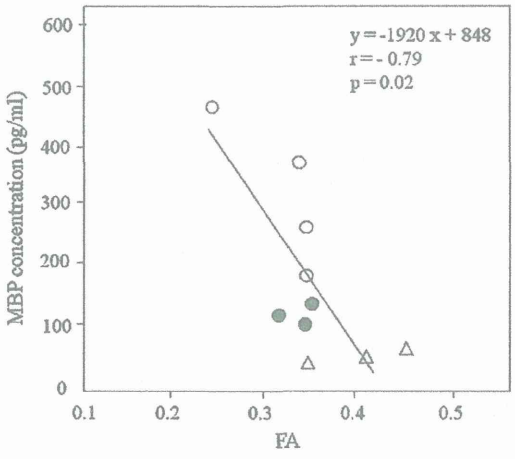

Fig. 3 Correlation between FA and MBP concentration in ten patients showing MBP concentration >40 pg/ml. *White circle*, patient with persistent chronic symptoms in group S; *black circle*, patient with DNS in group S; *triangle*, patient in group A

The timing for MBP measurements in the present study was thus established at 2 weeks (between day 12 and day 16) after admission. As a result, the incidence of abnormal MBP concentration was significantly higher in patients with chronic neuropsychiatry symptoms (group S) than in patients without chronic symptoms (group A) or controls. These results suggest that patients in group S certainly suffered from demyelinating changes somewhere in the CWM and support the theory that chronic neuropsychiatric symptoms after CO intoxication result from progressive demyelination in the CWM [24, 25]. The MBP concentration in case 6 was slightly lower (99 pg/ml) than the abnormal level, but the patient displayed akinetic mutism compatible with DNS at 1 week after measurement of MBP. The concentration of MBP in this patient might have been on the way to reaching abnormal levels, as demyelination of CWM in patients with DNS has been considered to undergo gradual progression during the lucid interval [13]. MBP concentrations of DNS patients were between those of patients with persistent symptoms in group S and those of patients in group A (Table 1; Fig. 3). These findings may indicate that demyelination begins to progress during the lucid interval before DNS. Although measuring MBP concentrations thus offers a useful indicator for assessing the extent of demyelination due to CO poisoning, detection of MBP using a lumbar tap is a highly invasive procedure and only indicates white-matter damage somewhere within the CNS.

Neuroimaging is minimally invasive and can visualize any region in the CWM. T2-weighted imaging (T2WI) often depicts abnormalities in the CWM in CO-poisoned patients. However, the interpretation of findings from routine MRI is difficult, as hyperintense foci in the CWM on T2WI can represent various progressive histological changes, including vasogenic edema, multiple necrosis, extensive axonal destruction and/or demyelination without axonal destruction [4, 12]. We therefore performed DTI in the same period as detection of MBP, since DTI is potentially more sensitive for assessing the extent of demyelinating changes in the CWM than other MRI sequences. As progressive reduction of FA values with age has been reported [5], we compared patients <60 years old with age-matched controls in this study. The finding of no significant difference in mean age among groups S, group A and controls suggests a negligible contribution of aging to FA values in this study. Previous reports have documented damage in various regions of the CWM after CO poisoning [8, 18, 28]. Indeed, some studies have reported correlations between FA values in various regions of the CWM in the chronic phase and cognitive dysfunction among CO-poisoned patients with DNS [16, 23, 30]. However, the centrum semiovale in the CWM has been suggested as a key region responsible for chronic neurological symptoms [4, 10, 19, 22]. A study using DTI at various phases after CO poisoning has also shown that FA in the centrum semiovale changes in parallel with cognitive impairments or neurological symptoms [17]. Based on these reports, we placed the ROI on the centrum semiovale to measure FA and ADC from DTI. As a result, mean FA for group S presenting with chronic neuropsychiatric symptoms was significantly lower than that for group A presenting with no chronic symptoms or that for controls consisting of healthy volunteers, whereas no significant difference was evident between group A and controls. In contrast, mean ADC did not differ significantly among the three groups. FA must be more sensitive for detecting CWM damage than ADC. Furthermore, these findings suggest that white matter fibers in the centrum semiovale were demyelinated in the subacute phase (2 weeks after poisoning) in CO-poisoned patients presenting with chronic symptoms. Notably, reductions in FA, suggestive of demyelination, were already present in the centrum semiovale before the recurrence of symptoms in the three patients with DNS. The reliability of this finding is supported by the result that MBP concentrations in DNS patients showed greater increases than those in group A patients at 2 weeks. These findings indicate the possibility of using FA in the centrum semiovale as an appropriate examination for predicting DNS during the lucid interval.

Our pilot study of DTI for CO-poisoned patients showed that FA enables representation of damage to white matter fibers in the centrum semiovale of patients with chronic neuropsychiatric symptoms [3]. That report, however, failed to demonstrate any correlation between FA in the centrum semiovale and MBP concentration, presumably because of the small sample size. Although subject criteria

were more strictly established in the present study than in our previous investigation, the greater number of subjects in this study allow us to show a linear correlation between FA and MBP in ten patients showing MBP concentrations >40 pg/ml. This finding validated the use of the centrum semiovale to represent various demyelinated lesions in the CWM, and FA in the centrum semiovale obviously offers a quantitative indicator of demyelination in CO-poisoned patients with chronic neuropsychiatric symptoms.

Some limitations must be considered in the interpretation of the study results. First, FA in the centrum semiovale may not strictly mirror the amount of demyelination in the whole CWM, although FA in the centrum semiovale correlated with MBP concentration. In group S, FA values in the centrum semiovale of the three DNS patients were not clearly different from those of the four patients with persistent symptoms (Fig. 2a), whereas MBP seemed to allow differentiation between subgroups in group S (around 100 pg/ml in patients with DNS and ≥150 pg/ml in patients with persistent chronic symptoms). This discrepancy might hypothetically be explained if demyelinated lesions in patients with persistent symptoms vary more than those in DNS patients. FA measured in this study suggests the magnitude of demyelination in the centrum semiovale, whereas MBP concentration not only indicates the magnitude, but also the width of demyelination in the whole CNS. We think that FA in the centrum semiovale cannot allow differentiation of the severity of CWM damage among subjects including patients with DNS and those with persistent symptoms. Second, the chronic neuropsychiatric symptoms seen after CO poisoning may not be solely attributable to demyelinating changes in fibers of the centrum semiovale. However, knowing to the focus on the region of the CWM is obviously very useful when evaluating the extent of CO-induced CWM damage using neuroimaging. We considered that the centrum semiovale represents the main region of damage and should be the focus of attention on neuroimaging in the subacute phase after CO poisoning [10]. Third, the sample size in this study was still small, with markedly fewer subjects in group S than in group A. The small number of DNS patients resulted in difficulties with statistical comparisons between subgroups in group S and other groups. However, the small sample size resulted from the strict entry criteria for this study. Furthermore, we did not select subjects with any bias other than the criteria established for this study. Indeed, percentages for patients with and without chronic symptoms in this study were in agreement with the results of previous reports [6, 33]. Fourth, findings in this study cannot be applied to patients over 60 years old. In senior patients, FA values may be overestimated as aging may lead to reduced FA values.

Conclusions

This is the first report to find that FA in the CWM correlates with MBP concentrations in the CSF during the subacute phase in CO-poisoned patients. The identification of a significant negative correlation between FA in the centrum semiovale and MBP concentration validates the concept that the centrum semiovale can reveal various demyelinated lesions in the CWM and that FA in the centrum semiovale offers a quantitative indicator of demyelination in CO-poisoned patients with chronic neuropsychiatric symptoms.

Acknowledgments This study was supported in part by a Grant-in-Aid for Scientific Research (C) and for the Strategic Medical Science Research Center for Advanced Medical Science Research from the Ministry of Science, Education, Sports and Culture, Japan.

Conflicts of interest None.

References

1. Bammer R, Augustin M, Strasser-Fuchs S, Seifert T, Kapeller P, Stollberger R, Ebner F, Hartung HP, Fazekas F (2000) Magnetic resonance diffusion tensor imaging for characterizing diffuse and focal white matter abnormalities in multiple sclerosis. Magn Reson Med 44:583–591
2. Beaulieu C (2002) The basis of anisotropic water diffusion in the nervous system—a technical review. NMR Biomed 15:435–455
3. Beppu T, Nishimoto H, Ishigaki D, Fujiwara S, Yoshida T, Oikawa H, Kamada K, Sasaki M, Ogasawara K (2010) Assessment of damage to cerebral white matter fiber in the subacute phase after carbon monoxide poisoning using fractional anisotropy in diffusion tensor imaging. Neuroradiology 52:735–743
4. Chang KH, Han MH, Kim HS, Wie BA, Han MC (1992) Delayed encephalopathy after acute carbon monoxide intoxication: MR imaging features and distribution of cerebral white matter lesions. Radiology 184:117–122
5. Charlton RA, Barrick TR, McIntyre DJ, Shen Y, O'Sullivan M, Howe FA, Clark CA, Morris RG, Markus HS (2006) White matter damage on diffusion tensor imaging correlates with age-related cognitive decline. Neurology 66:217–222
6. Choi IS (1983) Delayed neurologic sequelae in carbon monoxide intoxication. Arch Neurol 40:433–435
7. Ernst A, Zibrak JD (1998) Carbon monoxide poisoning. N Engl J Med 339:1603–1608
8. Fan HC, Wang AC, Lo CP, Chang KP, Chen SJ (2009) Damage of cerebellar white matter due to carbon monoxide poisoning: a case report. Am J Emerg Med 27(757):e755–e757
9. Folstein MF, Folstein SE, McHugh PR (1975) "Mini-mental state". A practical method for grading the cognitive state of patients for the clinician. J Psychiatr Res 12:189–198
10. Fujiwara S, Beppu T, Nishimoto H, Sanjo K, Koeda A, Mori K, Kudo K, Sasaki M, Ogasawara K (2011) Detecting damaged regions of cerebral white matter in the subacute phase after carbon

monoxide poisoning using voxel-based analysis with diffusion tensor imaging. Neuroradiology. doi:10.1007/s00234-011-0958-8
11. Ide T, Kamijo Y (2008) Myelin basic protein in cerebrospinal fluid: a predictive marker of delayed encephalopathy from carbon monoxide poisoning. Am J Emerg Med 26:908–912
12. Jain K (2009) Carbon monoxide and other tissue poisons. In: Jain KK (ed) Textbook of hyperbaric medicine, 5th edn. Hogrefe and Huber Publisher, Massachusetts, pp 43–133
13. Kado H, Kimura H, Murata T, Itoh H, Shimosegawa E (2004) Carbon monoxide poisoning: two cases of assessment by magnetization transfer ratios and 1H-MRS for brain damage. Radiat Med 22:190–194
14. Kamijo Y, Soma K, Ide T (2007) Recurrent myelin basic protein elevation in cerebrospinal fluid as a predictive marker of delayed encephalopathy after carbon monoxide poisoning. Am J Emerg Med 25:483–485
15. Lapresle J, Fardeau M (1967) The central nervous system and carbon monoxide poisoning. II. Anatomical study of brain lesions following intoxication with carbon monixide (22 cases). Prog Brain Res 24:31–74
16. Lin WC, Lu CH, Lee YC, Wang HC, Lui CC, Cheng YF, Chang HW, Shih YT, Lin CP (2009) White matter damage in carbon monoxide intoxication assessed in vivo using diffusion tensor MR imaging. AJNR Am J Neuroradiol 30:1248–1255
17. Lo CP, Chen SY, Chou MC, Wang CY, Lee KW, Hsueh CJ, Chen CY, Huang KL, Huang GS (2007) Diffusion-tensor MR imaging for evaluation of the efficacy of hyperbaric oxygen therapy in patients with delayed neuropsychiatric syndrome caused by carbon monoxide inhalation. Eur J Neurol 14:777–782
18. O'Donnell P, Buxton PJ, Pitkin A, Jarvis LJ (2000) The magnetic resonance imaging appearances of the brain in acute carbon monoxide poisoning. Clin Radiol 55:273–280
19. Parkinson RB, Hopkins RO, Cleavinger HB, Weaver LK, Victoroff J, Foley JF, Bigler ED (2002) White matter hyperintensities and neuropsychological outcome following carbon monoxide poisoning. Neurology 58:1525–1532
20. Prockop LD, Chichkova RI (2007) Carbon monoxide intoxication: an updated review. J Neurol Sci 262:122–130
21. Shrout PE, Fleiss JL (1979) Intraclass correlations: uses in assessing rater reliability. Psychol Bull 86:420–428
22. Sohn YH, Jeong Y, Kim HS, Im JH, Kim JS (2000) The brain lesion responsible for parkinsonism after carbon monoxide poisoning. Arch Neurol 57:1214–1218
23. Terajima K, Igarashi H, Hirose M, Matsuzawa H, Nishizawa M, Nakada T (2008) Serial assessments of delayed encephalopathy after carbon monoxide poisoning using magnetic resonance spectroscopy and diffusion tensor imaging on 3.0T system. Eur Neurol 59:55–61
24. Thom SR (1990) Carbon monoxide-mediated brain lipid peroxidation in the rat. J Appl Physiol 68:997–1003
25. Thom SR, Bhopale VM, Fisher D, Zhang J, Gimotty P (2004) Delayed neuropathology after carbon monoxide poisoning is immune-mediated. Proc Natl Acad Sci USA 101:13660–13665
26. Thom SR, Bhopale VM, Han ST, Clark JM, Hardy KR (2006) Intravascular neutrophil activation due to carbon monoxide poisoning. Am J Respir Crit Care Med 174:1239–1248
27. Tievsky AL, Ptak T, Farkas J (1999) Investigation of apparent diffusion coefficient and diffusion tensor anisotrophy in acute and chronic multiple sclerosis lesions. AJNR Am J Neuroradiol 20:1491–1499
28. Uchino A, Hasuo K, Shida K, Matsumoto S, Yasumori K, Masuda K (1994) MRI of the brain in chronic carbon monoxide poisoning. Neuroradiology 36:399–401
29. Valk J, van der Knaap MS (1992) Toxic encephalopathy. AJNR Am J Neuroradiol 13:747–760
30. Vila JF, Meli FJ, Serqueira OE, Pisarello J, Lylyk P (2005) Diffusion tensor magnetic resonance imaging: a promising technique to characterize and track delayed encephalopathy after acute carbon monoxide poisoning. Undersea Hyperb Med 32:151–156
31. Weaver LK (2009) Clinical practice. Carbon monoxide poisoning. N Engl J Med 360:1217–1225
32. Weaver LK, Hopkins RO, Chan KJ, Churchill S, Elliott CG, Clemmer TP, Orme JF Jr, Thomas FO, Morris AH (2002) Hyperbaric oxygen for acute carbon monoxide poisoning. N Engl J Med 347:1057–1067
33. Weaver LK, Hopkins RO, Elliott G (1999) Carbon monoxide poisoning. N Engl J Med 340:1290 Author reply 1292
34. Zagami AS, Lethlean AK, Mellick R (1993) Delayed neurological deterioration following carbon monoxide poisoning: MRI findings. J Neurol 240:113–116
35. Zhang J, Piantadosi CA (1992) Mitochondrial oxidative stress after carbon monoxide hypoxia in the rat brain. J Clin Invest 90:1193–1199